Quantitative profiling of endocannabinoids and related *N*-acylethanolamines in human CSF using nano LC-MS/MS[s]

Vasudev Kantae,[1,]* Shinji Ogino,[1,2,]* Marek Noga,[3,]* Amy C. Harms,* Robin M. van Dongen,[†] Gerrit L. J. Onderwater,[†] Arn M. J. M. van den Maagdenberg,[†,§] Gisela M. Terwindt,[†] Mario van der Stelt,** Michel D. Ferrari,[†] and Thomas Hankemeier[4,]*

Division of Analytical Biosciences, Leiden Academic Centre for Drug Research* and Department of Bioorganic Synthesis, Leiden Institute of Chemistry,** Leiden University, Leiden, The Netherlands; and Departments of Neurology[†] and Human Genetics,[§] Leiden University Medical Center, Leiden, The Netherlands

ORCID IDs: 0000-0001-8541-0882 (V.K.)

Abstract Endocannabinoids, a class of lipid messengers, have emerged as crucial regulators of synaptic communication in the CNS. Dysregulation of these compounds has been implicated in many brain disorders. Although some studies have identified and quantified a limited number of target compounds, a method that provides comprehensive quantitative information on endocannabinoids and related *N*-acylethanolamines (NAEs) in cerebrospinal fluid (CSF) is currently lacking, as measurements are challenging due to low concentrations under normal physiological conditions. Here we developed and validated a high-throughput nano LC-ESI-MS/MS platform for the simultaneous quantification of endocannabinoids (anandamide and 2-arachidonoylglycerol), ten related NAEs, and eight additional putatively annotated NAEs in human CSF. Requiring only 200 µl of CSF, our method has limits of detection from 0.28 to 61.2 pM with precisions of relative SD <15% for most compounds. We applied our method to CSF from 45 healthy humans and demonstrated potential age and gender effects on concentrations of endocannabinoids and NAEs. Notably, our results show that docosahexaenoylethanolamide concentrations increase with age in males. **jlr** Our method may offer new opportunities to gain insight into regulatory functions of endocannabinoids in the context of (ab)normal brain function.—Kantae, V., S. Ogino, M. Noga, A. C. Harms, R. M. van Dongen, G. L. J. Onderwater, A. M. J. M. van den Maagdenberg, G. M. Terwindt, M. van der Stelt, M. D. Ferrari, and T. Hankemeier. **Quantitative profiling of endocannabinoids**

and related *N*-acylethanolamines in human CSF using nano LC-MS/MS. *J. Lipid Res.* 2017. **58:** 615–624.

The endocannabinoid system has emerged as a crucial regulator of synaptic communication in the CNS (1–3). Dysregulation of this system is implicated in various neurological and psychiatric disorders, such as neuroinflammation, stroke, brain trauma, anxiety, and depression (4–8). The endocannabinoid system consists of endogenous lipid messengers (endocannabinoids) that activate two distinct cannabinoid (CB) (CB$_1$ and CB$_2$) receptors and the enzymes responsible for the synthesis and degradation of the endocannabinoids. Anandamide (AEA; *N*-arachidonoyl

ethanolamine) and 2-arachidonoylglycerol (2-AG) are the two best studied endocannabinoids (9). They are synthesized on demand from membrane lipids in a stimulus-dependent manner and are degraded by fatty acid amide hydrolase (FAAH) and monoacylglycerol lipase (MAGL), respectively (10, 11).

In addition to AEA and 2-AG, there are endogenous lipid compounds capable of activating the CB_1 and CB_2 receptors, i.e., virodhamine [O-arachidonoyl ethanolamine (O-AEA)], N-arachidonoyldopamine (NADA), and noladinether [2-arachidonylglycerol ether (2-AGE)], but their physiological relevance is largely unknown. Related bioactive lipids, such as N-linoleoylethanolamine (LEA), N-palmitoylethanolamine (PEA), N-oleoylethanolamine (OEA), and N-stearoylethanolamine (SEA) are produced through the same biosynthetic pathway as AEA. These N-acylethanolamines (NAEs) have negligible or only weak affinity for the CB_1 and CB_2 receptors, but are able to indirectly modulate CB receptor activity by interfering with endocannabinoid metabolism, the so-called "entourage effect" (12). Of note, some of the NAEs may exert biological activities through other proteins, such as transient receptor potential cation channel subfamily V member 1 (TRPV1), G-coupled protein receptors (GPR55, GPR18, and GPR119), or nuclear receptors (peroxisome proliferator-activated receptors α and γ) (13, 14). It is worth mentioning that the endocannabinoids, arachidonoylglycerols, and fatty acid ethanolamides are not only metabolized by FAAH or MAGL, but are oxidized by several other enzymes, such as cyclo-oxygenase-2 (COX-2), cytochrome P450, and lipoxygenase (LOX) enzymes. These enzymes convert endocannabinoids into a new array of oxygenated intermediates, such as prostaglandin ethanolamides (called as prostamides) and prostaglandin glycerol esters, or the lipids can be lipoxygenated to many hydroxylated end-products. However, these intermediates are pharmacologically distinct from their parent endocannabinoids and possess different biological functions (15, 16).

Quantification of endocannabinoid levels in the CNS is important to understand their role in human brain disease. Because the cerebrospinal fluid (CSF) is exchanged with brain interstitium, it is regarded as the most relevant accessible body fluid that reflects free endocannabinoid and NAE levels in the CNS (17). However, limited information is currently available on endocannabinoid and NAE levels in the CSF from healthy humans or patients. Previous studies have quantified the endocannabinoids, 2-AG and AEA (18–21), and two NAEs (OEA and PEA) (22–24), but not the related lipid messengers.

Under normal physiological conditions, endocannabinoid concentrations are very low (in the nanomolar to femtomolar range) in CSF compared with their levels in blood and tissues. This puts extra demands on the sensitivity of the quantification method. Advanced powerful techniques, such as ultra-HPLC, coupled to MS have been employed to quantify endocannabinoids in blood (25–27) and other tissue extracts (28), but these techniques are less suitable for endocannabinoid quantification in CSF due to its limited availability. We envisioned that nano LC would offer the opportunity to increase the sensitivity of the analytical system; a microfluidic chip-based approach would provide the required sensitivity by allowing injection of a larger sample volume by coupling an on-line enrichment column to a small internal diameter analytical column, resulting in a higher concentration in the eluting peak. In addition, the reduced flow rate of nano LC compared with conventional LC can improve sensitivity through an increase in the ionization efficiency (29). Using microfluidic chip-based technology, incorporating an enrichment column, a six-port valve, a separation column, and a nano electrospray tip allows the coupling of miniaturized separation with a nano ESI source (30). This design results in lower dead volumes and fewer connections compared with classical nano LC equipment, thereby leading to increased sensitivity and robustness by less peak broadening and dilution effects during transfer of the sample to the LC column and later to the LC-MS interface (31).

By making use of these advantages, we developed and validated a nano LC-ESI-MS/MS method for the simultaneous quantification of endocannabinoid and related NAEs in clinical (human) CSF. By combining a simple liquid-liquid extraction method for sample preparation, a nano LC separation, and multiple reaction monitoring (MRM) for detection, we could show that an extended range of endocannabinoids and related molecules can be measured. To show the applicability of this novel method, CSF samples of 45 healthy volunteers were measured to study variation in endocannabinoid levels in relation to gender and age.

MATERIAL AND METHODS

Materials

UPLC-grade acetonitrile (ACN) and methanol (MeOH) were purchased from Actu-All Chemicals (Oss, The Netherlands). Formic acid was purchased from Acros Organics (Morris Plains, NJ). Toluene was obtained from Biosolve (Valkenswaard, The Netherlands). EDTA disodium salt was obtained from Sigma-Aldrich Chemie B.V. (Zwijndrecht, The Netherlands). Purified Millipore water was obtained from a Milli-Q PF Plus system (Merck Millipore). NADA, 1-AG, 2-AG, N-docosatetraenoylethanolamide (DEA), N-docosahexaenoylethanolamide (DHEA), 2-AGE, N-dihomo-γ-linolenoylethanolamide (DGLEA), AEA, SEA, OEA, LEA, PEA, O-AEA, and deuterated standards, NADA-d8, 2-AG-d8, DHEA-d4, AEA-d8, SEA-d3, OEA-d4, LEA-d4, and PEA-d4 were purchased from Cayman Chemical (Ann Arbor, MI).

Preparation of standards and internal standards

Pure standards (>98% purity) in ethanol or ACN at different stock concentrations were provided from the manufacturer. The standard stock solutions were diluted to a concentration of 1 mM using ACN. A final mix of working solution at 100 nM for compounds in group A (NADA, AEA, DEA, DHEA, DGLEA, 2-AGE, LEA, and O-AEA) and at 1,000 nM for compounds in group B (2-AG, 1-AG, SEA, OEA, and PEA) were prepared. The deuterated internal standard (ISTD) solutions were diluted to 100 μM except for 2-AG-d8 at 259 μM. A final working solution was prepared with 100 nM AEA-d8, NADA-d8, DHEA-d4 and 1,000 nM 2-AG-d8, SEA-d3, PEA-d4, LEA-d3, and OEA-d4.

Calibration curve preparation

On the day of analysis, the standard working solution was further diluted to seven additional calibration levels as shown in **Table 1**. Each calibration point was mixed with ISTD-mix at a 1:1 ratio. The concentrations of ISTDs were chosen to be near the endogenous concentrations of the analytes in CSF.

Sampling protocol for clinical CSF samples used for method development and validation

CSF was sampled via lumbar puncture between L3/L4, L4/L5, or L5/S1. CSF was collected in 12 ml polystyrene tubes (numbers 160172 and 160172; Greiner Bio-One B.V., Alphen aan den Rijn, The Netherlands) and processed within 30 min. A small portion was used for cell count, and the remaining CSF was centrifuged at 21°C for 5 min (500 *g*). A portion of the supernatant was used for clinical measurements (i.e., glucose, total protein), and the remaining CSF was stored in 2.0 ml polyethylene cryotubes (Micro tube, number 72609; Sarstedt AG and Co., Nümbrecht, Germany) and stored at −20°C. All samples remained at −20°C until they were pooled in a 50 ml polypropylene tube (number 210261; Greiner Bio-One B.V). The pooled sample was aliquoted into 2 ml Eppendorf tubes (number 211-2120; VWR, Amsterdam, The Netherlands) and stored at −80°C. These clinical CSF samples were used for the purpose of method validation and are termed "pooled CSF samples". On the day of analysis, 1,000 µl of ethanol was added to each aliquot (0.5 ml CSF) to model conditions of study samples, mixed thoroughly, and placed on ice.

Sampling of healthy subjects

CSF study samples were collected for an ongoing biochemical study, which was approved by the local medical ethics committee (LUMC). All subjects provided written informed consent before sampling. Prior to CSF sampling, 6 ml of cold ethanol (ethanol absolute, number 8098; J.T. Baker, Phillipsburg, NJ) was added to a 15 ml polypropylene sampling tube (number 188271; Greiner Bio-One B.V.) and placed on ice. Ethanol was added for denaturation of enzymes present in CSF upon sampling. Subsequently, 3 ml of CSF was sampled directly into the tube and inverted several times to mix CSF and ethanol thoroughly. Immediately after sampling, the CSF/ethanol mixture was divided in 1.5 ml aliquots into 7 × 1.8 ml cryotubes (number 368632; Nunc, Hardenberg, The Netherlands) and placed on dry ice within 30 min from sampling. All aliquots were stored at −80°C within 60 min from sampling. No extra freeze-thaw cycles were allowed before sample preparation.

Sample extraction

Sample extraction was performed on ice. For CSF samples, 600 µl of the CSF/ethanol mixture (200 µl/400 µl) was transferred into 2 ml Eppendorf tubes and 100 µl of 100 mM citrate buffer (pH 5.0) with 25 mM EDTA and 10 µl of deuterated ISTD mixture were added. After adding 550 µl of ice-cold toluene, the tubes were thoroughly mixed for 3 min using a bullet blender (Next Advance, Inc., Averill Park, NY), followed by a centrifugation step (4°C, 5,000 *g*, 5 min). Then 475 µl of the upper layer (toluene)

were aspirated and transferred into 500 µl Eppendorf tubes. Samples were dried under a gentle stream of nitrogen and placed on ice followed by reconstitution with 10 µl of water/MeOH (50/50). The reconstituted samples were centrifuged (4°C, 10,000 *g*, 5 min) before transferring into vials for LC-MS.

Chip-based nano LC-MS/MS analysis

Endocannabinoids and related NAEs were measured using a targeted method on an Agilent 6460 triple quadrupole MS system in conjunction with an Agilent 1100/1200 series nano-LC system consisting of a G1375 capillary pump, a G2226 nano pump, and a G1376 uWPS autosampler with thermostat (Agilent Technologies, Waldbron, Germany). Separation was carried out with an Agilent Polaris-HR-Chip 3C18 (G4240-62030), which was inserted in the HPLC-Chip Cube MS interface (Agilent Technologies) operated at ambient temperatures. This chip has a 360 nL enrichment column with a 150 mm (length) × 75 µm (width) separation column and a particle size of 3 µm. The mobile phase was 10 mM formic acid/water (A) and ACN (B). The analytical gradient was performed in two steps: first, 8 µl of sample were loaded on the enrichment column using the capillary pump delivering a mobile phase in isocratic mode composed of 40% B at a flow rate of 2 µl/min. After the sample was trapped on the enrichment column, it was switched in line with the analytical column. The nano pump gradient started at 45% B and linearly increased up to 80% B in 12 min at a flow rate of 400 nl/min. The column was then held at 95% B for 2 min before returning to 45% B. The column was re-equilibrated for 5 min prior to the next injection, giving a total analysis time of 20 min. During the analytical gradient, the enrichment column was flushed with 16 µl of 100% B for 8 min. At the same time, the injection needle was washed with ACN/water (1/1, v/v) using an injection program. The temperature in the autosampler was maintained at 8°C. ESI was operated in positive ion mode with a capillary spray voltage set at 1,800 V and nitrogen nebulizer gas flow rate of 4 l/min and a temperature of 365°C. For endocannabinoids and related NAEs, individually optimized MRM parameters were determined for each transition for target compounds and ISTDs. The detailed list of MRM parameters and transitions is shown in supplemental Table S1.

To maximize the potential of the platform, MRM transitions for other NAEs were also included. Targets were selected based on: *1)* combinations of major fatty acids and ethanolamine (general structure of NAEs) and *2)* measurements of CSF by precursor ion scan mode for the characteristic product ion of NAEs, which is the protonated ethanolamine ion at *m/z* 62 (data not shown). These putatively annotated NAEs are listed as EA (from ethanolamine) followed by a molecular mass (*m/z*) value. Details of MRM transitions included in the method are listed in supplemental Table S1.

Data preprocessing

Peak area integration was performed with Mass Hunter quantitative analysis (version B.05.01; Agilent, Santa Clara, CA) and manually inspected. Peak areas of analytes were corrected by the

TABLE 1.   Stock concentrations of endocannabinoids and related NAE standards in the calibration line

Compound Group	Concentrations (nM)[a]							
	C0	C1	C2 (Low)	C3	C4 (Medium)	C5	C6 (High)	C7
A	0	0.01	0.03	0.1	0.3	1	3	10
B	0	0.1	0.3	1	3	10	30	100

[a]Seven levels of standard solutions (C1 to C7) are spiked to build the calibration line. These standards will be diluted 21 times in CSF matrix for their final concentrations.

appropriate ISTD and response ratios were calculated and used throughout the analysis.

Method validation

An in-house 3 day validation protocol was used to determine linearity, limit of detection (LOD), limit of quantification (LOQ), precision (intra- and inter-batch effect), recovery, and matrix effect (32).

Linearity, LOD, and LOQ. Purchased standards were spiked to both pooled CSF ("matrix calibration line") and water as blank matrix ("academic calibration line") in seven different concentrations (Table 1) to determine the linearity, LOD, and LOQ. For method validation, each calibration level was prepared using the sample extraction method explained above four times and injected once from each sample. Responses in the calibration levels were compared by means of *t*-tests going from low-level to high level. If there was no significant difference between two adjacent levels, then the lower level was excluded from the calibration curve. Regression lines for both matrix and academic line were calculated with $1/X^2$ weighting. If the differences in slopes of the regression lines between matrix and academic lines were less than 10%, LOD and LOQ values were calculated from academic lines. When the slopes differed, the matrix line was used for these calculations. Each LOD and LOQ was calculated as $3.3 \times$ (SD of *y*-estimate in the regression line/slope) and $3 \times$ LOD, respectively.

Precision. The intra-batch and inter-batch effects were evaluated using the quadruplicate analysis of the pooled CSF samples spiked at three different concentrations [lower level (C2), medium level (C4), and high level (C6)] over the three different days of the validation protocol. The pooled CSF was spiked with ISTDs, which behave like the endogenous compounds and are therefore perfectly suited to determine analytical characteristics. Precision was calculated as the relative SD (RSD) of the ratio of target to ISTD. An RSD less than 15% for medium and high levels and less than 20% for the low level was considered acceptable.

Recovery and matrix effect. Recovery and matrix effects were evaluated using ISTDs spiked to the pooled CSF samples. Recovery was assessed by determining the ratio of the peak areas obtained by spiking ISTDs to the sample before and after extraction. The matrix effect was assessed by determining the ratio of the peak areas obtained by spiking ISTDs to pooled CSF and to water after extraction.

Biological application in CSF of healthy subjects

A small study was performed to understand the changes in endocannabinoid levels in the CSF of healthy subjects due to gender and age. The experimental design included 45 individual study samples plus performance indicators. Duplicate samples were prepared and analyzed for five samples (15% of total samples). Additionally, 20 quality control (QC) samples were prepared by pooling individual study samples. A calibration curve was prepared by spiking the calibration standards along with ISTDs to the QC samples. All samples were randomized and each batch included calibration samples and an even distribution of duplicates, QC samples, and blanks.

Data pretreatment

To detect outliers among QC samples, a principle component analysis was used and QCs outside the 95% confidence region were detected and removed as statistical outliers. Two QC samples showed high concentrations for LEA, OEA, PEA, and SEA and were detected as statistical outliers. These concentrations were possibly caused by (an) exogenous source(s) (33). After removal of the outliers, the final QC set was used to determine optimal ISTDs for compounds without an isotopically labeled equivalent as an ISTD, as previously described (34). Values from QC samples were used for monitoring data quality and correcting for shifts in MS sensitivity over time (34). After correction with QC samples, RSDs of study QC samples were calculated for all compounds. Next, corrected data of biological samples (identified compounds only) were analyzed with principle component analysis to detect outliers. In the current data set, one outlier was detected and was removed from further statistical analysis. Finally, RSDs of duplicates were calculated and afterwards one of two samples was randomly selected from the remaining duplicate pairs to analyze variability. One duplicate pair was identified as an outlier due to contamination and was excluded.

Statistical analysis

Prior to statistical analysis, study QC-corrected data were log-transformed for data normalization. To study whether endocannabinoid and related NAE concentrations depend on gender or age, multiple linear regression analysis was applied. For each compound, its concentration was set as the dependent variable with gender and age as predictors. To study whether potential age effects are gender-specific, linear regression was repeated after splitting data by gender. Statistical analysis was performed with R software (version 3.0.3, function *lm*). All reported *P* values are without multiple testing corrections. $P < 0.05$ was considered significant.

RESULTS AND DISCUSSION

Method development

Although some analytical methods for profiling endocannabinoids and related NAEs in human plasma have been reported (25, 27), methods for CSF are limited to AEA, 2-AG, PEA, and OEA (22, 23). To achieve a high-throughput and sensitive method for detection and quantification of these compounds, two important parameters were optimized. First, LC conditions, including gradient and solvent composition, were optimized to obtain an adequate separation of molecules, especially isomers that are indistinguishable by fragmentation pattern, while at the same time maintaining a short chromatographic run time (**Fig. 1**). For example, DGLEA and EA350 are structural isomers, but are chromatographically separated (**Fig. 2**). Next, optimal transitions were determined for each compound to maximize sensitivity, and for each MS/MS transition it was confirmed with standards so that there was no cross-talk between compounds. This method uses dynamic MRM, which calculates optimal MRM parameters for multiple analytes using user inputs of retention time windows (delta RT) and cycle time and these parameters remain constant throughout all runs. The individual MRM dwell time is adjusted to maintain constant cycle time, which is selected to provide adequate sampling speed for quantitation of narrow LC peaks. When compared with traditional time segmented methods, dynamic MRM methods include fewer ion transitions per unit time during a typical MS
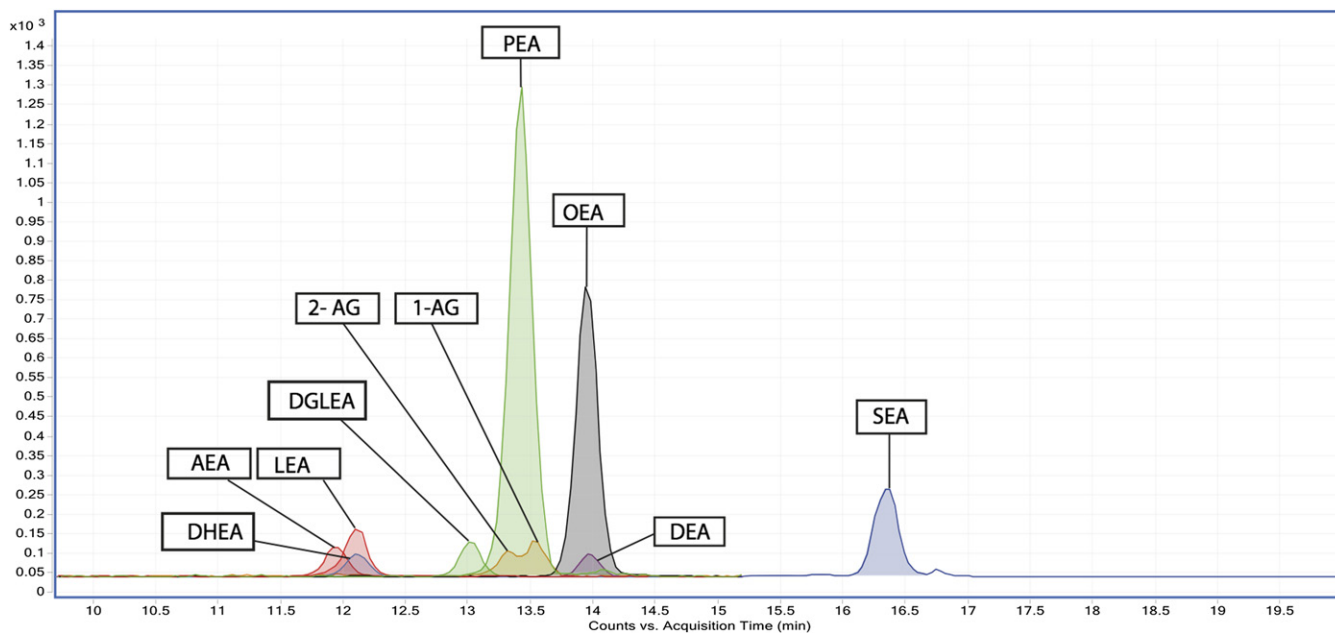
Fig. 1. Overlay of MS/MS chromatograms of endocannabinoids and related NAEs in standard mix.

scan, which results in longer dwell times for individual ion transitions. The MRM was operated in positive mode as the analytes were more efficiently ionized in that mode. For selective detection and quantification of co-eluting metabolites, specific precursor and fragment ions were used for their separation. The fragmentation pattern for NAE derivatives included the characteristic loss of m/z 62.1 resulting from the fragmentation of the amide bond (supplemental Fig. S3A). Our chip-based nano LC-MS/MS method allowed quantification of 12 endocannabinoids and related NAEs, along with eight putatively identified NAEs in CSF (supplemental Table S1).

The isomerization from 2-AG to 1-AG due to acyl migration complicates the measurements of the two regio-isomers. As shown in **Table 2**, the sum of 2-AG and 1-AG showed a superior RSD (5–11%) during batch measurement compared with 2-AG only (3–38%), which indicated that acyl migration might have occurred during sample preparation and measurement. Another contribution to that error could be problems with peak integration, as the two isomers are not separated at baseline. Based on this result, the sum of 1-AG and 2-AG was used for further data analysis in this work. In liquid-liquid extraction, toluene was previously reported to suppress acyl migration during the evaporation step to a large extent (35). However, moderate levels of acyl migration were observed in the current study and this is likely due to a difference in matrices and sample handling procedures compared with previous studies. Moreover, this is the first study to use a toluene extraction method for CSF; whereas, the previous studies were demonstrated in plasma (25, 35). Furthermore, it has been reported that elevated temperatures, presence of serum albumin in the sample, and high pH values accelerate acyl migration (35, 36). Interestingly, a recent study reports that, in plasma, 1-AG is not an endogenous compound, but

rather the result of chemical isomerization during sample storage and, therefore, summing the concentrations of both the isomers will provide meaningful data for biological interpretation (27).

It should be noted that nonnegligible amounts of SEA and, to a lesser extent, other NAEs (PEA, SEA, and OEA) were observed in the ethanol that was used during sample collection. This indicates that ethanol used in the sample collection protocol is a source of contaminants. We also observed contamination of NAEs, especially SEA, OEA, and PEA, at low levels when using MeOH instead of ACN (data not shown). However, only low levels of SEA compared with the endogenous concentration in CSF were seen in the blank (MeOH/water) showing the soundness of the analytical method (supplemental Fig. S1). The consequence of the contaminants present in ethanol, from solvents and other potential sources for PEA, SEA, and OEA, was a decline of analytical characteristics (linearity, LOD, LOQ, precision, recovery, and matrix effect). Previous studies identified basal concentrations of these compounds in organic solvents, plastics, and glassware (33). A recommendation to minimize contamination is to avoid addition of ethanol during CSF sampling or to check for contamination prior to use.

The stability of endocannabinoids and NAEs and their ex vivo generation, i.e., during and after sampling, needs greater attention to avoid variability and inaccuracy of the measurements. To date, the stability of endocannabinoids in CSF was not reported, but in blood, NAE concentrations dramatically increase when withdrawn blood samples are improperly stored. The 2-AG and 1-AG levels were shown to be stable for 2 h, but a gradual reduction of 2-AG was detected after 4 h (25). Here, the pooled CSF used for validation was not stored immediately at cold conditions after withdrawal, which might cause increased
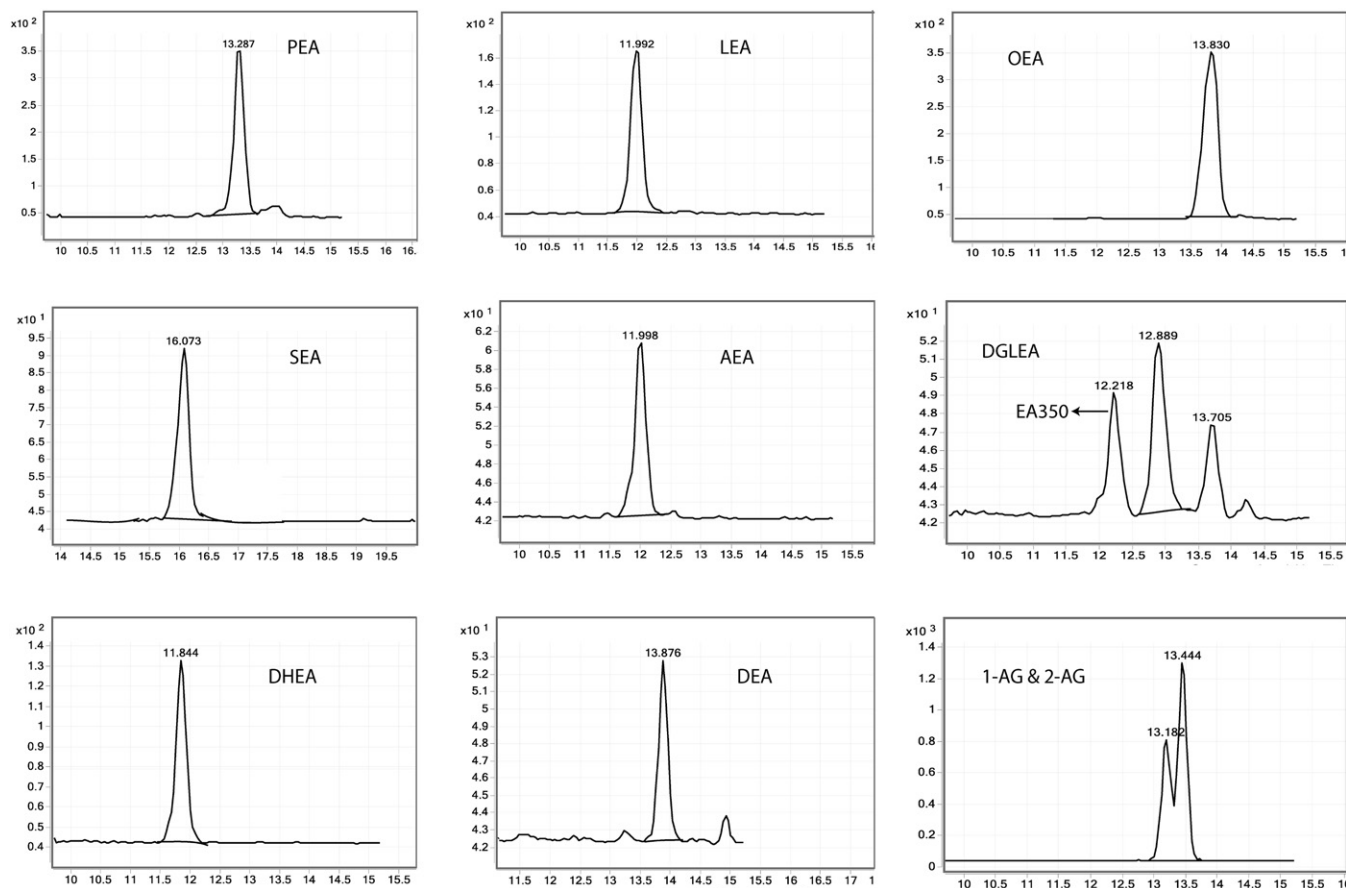
Fig. 2. Endogenous peaks of endocannabinoids and related NAEs in CSF. The x-axis is retention time and the y-axis is response signal.

NAE and 2-AG/1-AG levels. This has no negative consequences for this study because these pooled samples were only used to assess the validation parameters by spiking the ISTDs, and no biological conclusions were drawn from this pooled sample. The study samples, on the other hand, were processed and stored within 30 min after sample collection to improve the stability and accuracy of the measurements.

Method validation

Validation was performed using pooled CSF samples. Linearity and sensitivity (LOD and LOQ) are summarized in **Table 3**. Precision (intra- and inter-day) values are summarized in **Table 4**. Recovery and matrix effect are summarized in **Fig. 3**.

TABLE 2. Difference in percent RSD expressed in percentage between 2-AG alone and combined 2-AG and 1-AG

	RSD (%)	
Calibration Levels	2-AG	1-AG + 2-AG
C0	27	5
C1	38	8
C2	20	3
C3	15	11
C4	19	6
C5	16	8
C6	8	5
C7	3	4

Linearity and sensitivity. Pooled CSF samples were spiked with seven levels of calibration standards (Table 1) to determine linearity, LOD, and LOQ for each compound (nine targets). The goodness-of-fit, R^2, ranges from 0.995 to 0.999 for all compounds [with the exception of SEA (R^2 0.976)], demonstrating that the method is linear in the selected calibration range (supplemental Fig. S4). The LOQs are between 0.9 and 61.2 pM for most of the compounds, except for those with a contamination problem (PEA and SEA), which shows that the method is suitable for measuring endogenous levels in CSF (**Table 5**).

Precision. The intra- and inter-batch variability was assessed using the standards spiked at three different concentrations [low (C2), medium (C4), and high (C6)] in pooled CSF samples (Table 4). Quadruplicate sample preparations were performed in each batch, and a total of three batches were processed. The intra-batch RSDs ranged from 1% to 23%. Possible batch-to-batch effects were calculated using the three calibration levels (C2, C4, and C6) measured on three different days. Inter-batch effects ranged from 3% to 21%.

Recovery and matrix effect. Recovery and matrix effect were evaluated using deuterated compounds otherwise used as ISTDs (Fig. 3). Recovery was calculated as the ratio of the response of the ISTD of samples spiked before

TABLE 3. Validation parameters: calibration range, retention time, LODs, and LOQs

Compound	C	C=C	m/z	Calibration Ranges (pM)	Retention Time (min)	R^2	LOD (pM)	LOQ (pM)
PEA	16	0	299.5	4.7–4761	13.29	0.996	35.4	107.4
LEA	18	2	323.5	0.47–476	11.99	0.996	3.2	9.6
OEA	18	1	325.5	4.7–4761	13.83	0.997	14.4	43.7
SEA[a]	18	0	327.6	4.7–4761	16.07	0.976	146.9	445
AEA	20	4	347.5	0.47–476	12.00	0.997	0.28	0.86
DGLEA	20	3	349.6	0.47–476	12.89	0.996	0.53	1.6
DHEA	22	6	371.6	0.47–476	11.84	0.996	0.9	2.8
DEA	22	4	375.6	0.47–476	13.88	0.995	0.31	0.94
1-AG + 2-AG	20	4	378.6	4.7–4761	13.44 (1-AG) 13.18 (2-AG)	0.997	20.2	61.2

"C" and "C=C" are the number of carbon atoms and the number of double bonds in the fatty acid chain of the molecule, respectively. R^2, correlation coefficient.
[a]The LOD and LOQ values of SEA are high due to the contaminant peak present in ethanol added during sample collection.

extraction versus samples spiked after extraction. If possible losses of organic phase during sample extraction were compensated by using one of the deuterated ISTDs as ISTD (DHEA-d4), the recoveries were 81% to 119%. Matrix effect (ion suppression) was calculated as the ratio of the response of the ISTD spiked after extraction in matrix versus water. The matrix effect ranged from 38% to 81%. The ion suppression for these compounds most probably is due to co-eluting phospholipids. SEA-d3 was removed from Fig. 3 due to ion suppression by the presence of a high concentration of unlabeled SEA contamination in the sample collection solvents (see above). The compounds had good recovery after correction by an ISTD added prior to extraction. The matrix effects differed between compounds. This does not present a problem as long as an isotopically labelled compound is available as an ISTD; fortunately, for those compounds for which isotopically ISTDs were not available, the matrix effects were reproducible. For target compounds with matching ISTDs, the ISTD-corrected concentrations were shown to have acceptable reproducibility. Among the detected compounds in the current method, seven compounds have their respective deuterated ISTD for analytical corrections, but for DGLEA and DEA, deuterated standards were not available. For these compounds, LEA-d4 and AEA-d4, respectively, were chosen as their ISTDs due to their chemical similarly and their similar elution times.

CSF endocannabinoids and related NAEs in healthy subjects

To demonstrate the applicability of the method, we measured 45 human CSF samples from 22 healthy females (mean age 30.9 ± 12.8 years SD) and 23 healthy males (mean age 39.3 ± 16.5 years SD). Nine compounds were detected and quantified (Fig. 2).

Endogenous concentrations and ranges of endocannabinoids measured in healthy subjects are listed in Table 5. In addition, the RSDs of QCs and duplicates used during the analysis of healthy subjects are reported in Table 5. The concentrations of AEA and 2-AG are in line with the previous studies (37). In addition to the compounds shown in Table 3, several putatively annotated NAEs were observed in human CSF (supplemental Fig. S2). Of note, an interesting observation in the current CSF samples is the ratio of DHEA/AEA being around 10, which is contrary to plasma, where the ratio is almost equal to 1 (27). This could be because the availability of DHA is greater in CSF than arachidonic acid, precursors for DHEA and AEA, which are then processed downstream at equal rates. If this is not the case, this could indicate that the synthesizing enzymes have a preference for DHA to generate DHEA or, alternatively, it could be that AEA is a better substrate for FAAH than DHEA. However, further investigation is required to elucidate the exact reason, but this was not the main aim of this study.

TABLE 4. Analysis of pooled CSF samples showing precision (intra- and inter-batch effect)

Compound	Intra-batch Precision (%)			Inter-batch Precision (%)		
	Low (C2)	Middle (C4)	High (C6)	Low (C2)	Middle (C4)	High (C6)
PEA	9	8	3	14	13	4
LEA	23	12	11	21	18	7
OEA	9	8	5	13	12	5
SEA	14	7	9	15	17	7
AEA	6	5	6	6	6	5
DGLEA	14	5	10	13	5	8
DHEA	5	1	3	4	5	3
DEA	9	3	5	10	7	4
1-AG + 2-AG	11	5	2	14	9	11

The precision values are expressed in RSD. Low, middle, and high are three different concentrations (for concentrations see Table 1) used to show intra- and inter-batch precision.
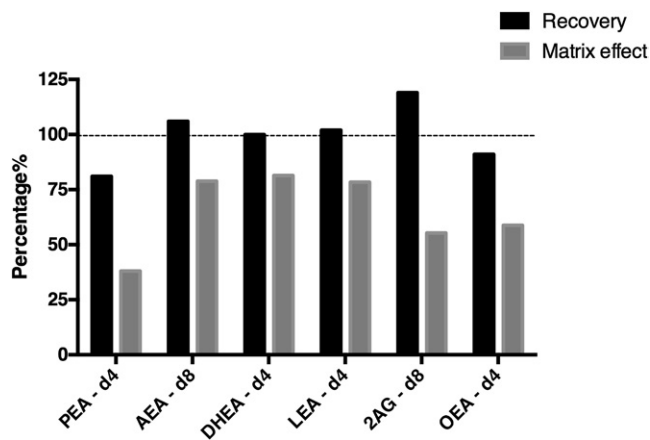
Fig. 3. Recovery and matrix effect of deuterated ISTDs in CSF. Recovery and matrix effect values are expressed in percentages. Recovery: higher values indicate better recoveries. Matrix effect: values above 100% imply ion enhancement and below 100% imply ion suppression.

The identity of one of the putatively annotated NAEs, EA350 peak, was assigned as 5(Z),8(Z),11(Z)-eicosatrienoic acid ethanolamide using a commercially available authentic standard and the identity was further confirmed by comparing *m/z*, retention time, and fragmentation pattern of the authentic standard. The MS/MS fragmentation is shown in supplemental Fig. S3B. In a similar manner, the identities of all the remaining putatively annotated NAEs should be confirmed by purchasing authentic standards; however, these standards are still not commercially available. Although further work needs to be done for annotating all metabolites and understanding the biological implications, this highly sensitive method clearly shows applicability in measuring a broad range of endocannabinoids and related NAEs.

Although we could not confirm the identity for most of the putatively identified compounds and observed some matrix effect due to ion suppression, we believe that our method with this broader coverage of endocannabinoids and their congeners will help us to understand the biological insights of the endocannabinoid system as a "whole" in future studies, and to possibly understand the biological role of these putatively identified compounds. Moreover, this method depicted acceptable reproducibility and sensi-

tivity of these molecules in the application to clinical samples, such as the migraine samples.

Gender and age differences in healthy controls

It is important for designing large case-control studies to know whether endocannabinoid and related NAE concentrations show a gender or age dependence. In our study, these factors were analyzed using data from healthy subjects using multiple linear regression analysis. Significant effects of age were present for DHEA. DHEA concentrations were higher in older males (**Fig. 4**). In blood, higher concentrations of DHA, the fatty acid of DHEA, were reported in the elderly (≥65 years, gender not reported) (38). Intake of DHA can alter DHEA concentrations in blood and brain (39). Additionally, age-related changes in DHA metabolism could play important roles as well (40). There were no significant gender differences in endocannabinoids or related NAEs when corrected for the age imbalance (supplemental Table S2). This study proves the importance of proper age and sex matching of cases and controls to obtain significant results in studies directed at discovery of endocannabinoid-related biomarkers and/or to obtain novel insights in health and disease.

CONCLUSIONS

A nano LC-ESI-MS/MS method for the simultaneous quantification of classical endocannabinoids and the related NAEs was developed and validated in human (clinical) CSF. We measured AEA, 2-AG, ten annotated NAEs, and eight putatively annotated NAEs, whereas previously only four endocannabinoids had been measured in CSF (22, 23). Requiring only 200 μl of CSF per sample, this sensitive method has LODs reaching picomolar-femtomolar levels, while maintaining good linearity and precision. Application of this method in CSF from healthy humans resulted in novel insights on gender and age effects, i.e., concentrations of DHEA increased with age in males, illustrating the possibilities of this method to study the regulatory functions of endocannabinoids in the context of brain (dys)function.

TABLE 5. Concentrations of endocannabinoids and related NAEs quantified in 45 CSF samples of healthy subjects with the RSD of QCs and duplicates

Compound Name	Concentration (pM)				QC_RSD (%) (n = 18)	Duplicate_RSD (%) (n = 4 Pairs)
	Minimum	Maximum	Median	SD		
PEA	41.4	270.4	83.7	48.7	10	48
LEA	3.6	28.8	9.6	6.2	10	33
OEA	22.0	116.6	44.4	19.0	15	20
SEA	67.0	310.3	108.4	54.5	13	57
AEA	0.5	2.7	1.6	0.5	10	14
DGLEA	0.4	2.2	1.0	0.4	5	6
DHEA	3.61	24.89	8.48	3.92	4	2
DEA	1.2	5.6	2.9	0.9	5	6
1-AG + 2-AG	36.5	235.3	82.6	44.7	11	6

The RSD expressed in percentage of QCs and duplicates used during the analysis of healthy subjects.
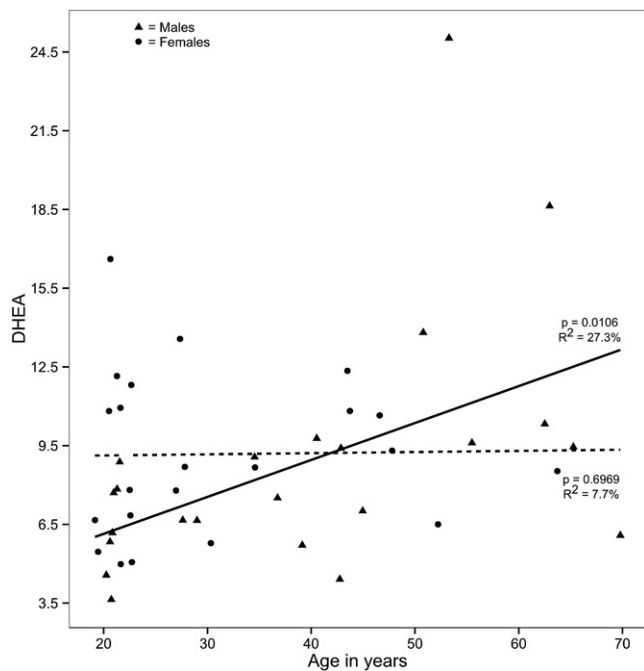
Fig. 4. Relationships between DHEA concentrations and age. Linear regression lines are plotted separately for males (solid line) and females (dotted line). Solid circles represent males and solid triangles represent females. The y-axis shows relative concentrations (in picomoles) before log transformation.

REFERENCES

1. Wilson, R. I., and R. A. Nicoll. 2002. Endocannabinoid signaling in the brain. *Science.* **296:** 678–682.
2. Di Marzo, V. 2011. Endocannabinoid signaling in the brain: biosynthetic mechanisms in the limelight. *Nat. Neurosci.* **14:** 9–15.
3. Freund, T. F., I. Katona, and D. Piomelli. 2003. Role of endogenous cannabinoids in synaptic signaling. *Physiol. Rev.* **83:** 1017–1066.
4. Di Marzo, V., N. Stella, and A. Zimmer. 2015. Endocannabinoid signalling and the deteriorating brain. *Nat. Rev. Neurosci.* **16:** 30–42.
5. Lutz, B., G. Marsicano, R. Maldonado, and C. J. Hillard. 2015. The endocannabinoid system in guarding against fear, anxiety and stress. *Nat. Rev. Neurosci.* **16:** 705–718.
6. Fernández-Ruiz, J., M. A. Moro, and J. Martínez-Orgado. 2015. Cannabinoids in neurodegenerative disorders and stroke/brain trauma: from preclinical models to clinical applications. *Neurotherapeutics.* **12:** 793–806.
7. Soltesz, I., B. E. Alger, M. Kano, S-H. Lee, D. M. Lovinger, T. Ohno-Shosaku, and M. Watanabe. 2015. Weeding out bad waves: towards selective cannabinoid circuit control in epilepsy. *Nat. Rev. Neurosci.* **16:** 264–277.
8. Katona, I., and T. F. Freund. 2008. Endocannabinoid signaling as a synaptic circuit breaker in neurological disease. *Nat. Med.* **14:** 923–930.
9. Mechoulam, R., L. O. Hanuš, R. Pertwee, and A. C. Howlett. 2014. Early phytocannabinoid chemistry to endocannabinoids and beyond. *Nat. Rev. Neurosci.* **15:** 757–764.
10. Di Marzo, V. 2008. Targeting the endocannabinoid system: to enhance or reduce? *Nat. Rev. Drug Discov.* **7:** 438–455.
11. Fowler, C. J. 2013. Transport of endocannabinoids across the plasma membrane and within the cell. *FEBS J.* **280:** 1895–1904.
12. Ho, W-S. V., D. A. Barrett, and M. D. Randall. 2008. "Entourage" effects of N-palmitoylethanolamide and N-oleoylethanolamide on vasorelaxation to anandamide occur through TRPV1 receptors. *Br. J. Pharmacol.* **155:** 837–846.
13. Bradshaw, H. B., and J. M. Walker. 2005. The expanding field of cannabimimetic and related lipid mediators. *Br. J. Pharmacol.* **144:** 459–465.
14. Tsuboi, K., N. Ikematsu, T. Uyama, D. G. Deutsch, A. Tokumura, and N. Ueda. 2013. Biosynthetic pathways of bioactive N-acylethanolamines in brain. *CNS Neurol. Disord. Drug Targets.* **12:** 7–16.
15. Urquhart, P., A. Nicolaou, and D. F. Woodward. 2015. Endocannabinoids and their oxygenation by cyclo-oxygenases, lipoxygenases and other oxygenases. *Biochim. Biophys. Acta.* **1851:** 366–376.
16. Rouzer, C. A., and L. J. Marnett. 2011. Endocannabinoid oxygenation by cyclooxygenases, lipoxygenases, and cytochromes P450: cross-talk between the eicosanoid and endocannabinoid signaling pathways. *Chem. Rev.* **111:** 5899–5921.
17. Brown, P. D., S. L. Davies, T. Speake, and I. D. Millar. 2004. Molecular mechanisms of cerebrospinal fluid production. *Neuroscience.* **129:** 957–970.
18. Koppel, J., H. Bradshaw, T. E. Goldberg, H. Khalili, P. Marambaud, M. J. Walker, M. Pazos, M. L. Gordon, E. Christen, and P. Davies. 2009. Endocannabinoids in Alzheimer's disease and their impact on normative cognitive performance: a case-control and cohort study. *Lipids Health Dis.* **8:** 2.
19. Romigi, A., M. Bari, F. Placidi, M. G. Marciani, M. Malaponti, F. Torelli, F. Izzi, C. Prosperetti, S. Zannino, F. Corte, et al. 2010. Cerebrospinal fluid levels of the endocannabinoid anandamide are reduced in patients with untreated newly diagnosed temporal lobe epilepsy. *Epilepsia.* **51:** 768–772.
20. Leweke, F. M., A. Giuffrida, D. Koethe, D. Schreiber, B. M. Nolden, L. Kranaster, M. A. Neatby, M. Schneider, C. W. Gerth, M. Hellmich, et al. 2007. Anandamide levels in cerebrospinal fluid of first-episode schizophrenic patients: impact of cannabis use. *Schizophr. Res.* **94:** 29–36.
21. Morgan, C. J., E. Page, C. Schaefer, K. Chatten, A. Manocha, S. Gulati, H. V. Curran, B. Brandner, and F. M. Leweke. 2013. Cerebrospinal fluid anandamide levels, cannabis use and psychotic-like symptoms. *Br. J. Psychiatry.* **202:** 381–382.
22. Jumpertz, R., A. Guijarro, R. E. Pratley, D. Piomelli, and J. Krakoff. 2011. Central and peripheral endocannabinoids and cognate acyl-ethanolamides in humans: association with race, adiposity, and energy expenditure. *J. Clin. Endocrinol. Metab.* **96:** 787–791.
23. Di Filippo, M., L. A. Pini, G. P. Pelliccioli, P. Calabresi, and P. Sarchielli. 2008. Abnormalities in the cerebrospinal fluid levels of endocannabinoids in multiple sclerosis. *J. Neurol. Neurosurg. Psychiatry.* **79:** 1224–1229.
24. Giuffrida, A., F. M. Leweke, C. W. Gerth, D. Schreiber, D. Koethe, J. Faulhaber, J. Klosterkötter, and D. Piomelli. 2004. Cerebrospinal anandamide levels are elevated in acute schizophrenia and are inversely correlated with psychotic symptoms. *Neuropsychopharmacology.* **29:** 2108–2114.
25. Fanelli, F., V. D. Di Lallo, I. Belluomo, R. De Iasio, M. Baccini, E. Casadio, D. I. Gasparini, M. Colavita, A. Gambineri, G. Grossi, et al. 2012. Estimation of reference intervals of five endocannabinoids and endocannabinoid related compounds in human plasma by two dimensional-LC/MS/MS. *J. Lipid Res.* **53:** 481–493.
26. Balvers, M. G. J., H. M. Wortelboer, R. F. Witkamp, and K. C. M. Verhoeckx. 2013. Liquid chromatography-tandem mass spectrometry analysis of free and esterified fatty acid N-acyl ethanolamines in plasma and blood cells. *Anal. Biochem.* **434:** 275–283.
27. Pastor, A., M. Farré, M. Fitó, F. Fernandez-Aranda, and R. de la Torre. 2014. Analysis of ECs and related compounds in plasma: artifactual isomerization and ex vivo enzymatic generation of 2-MGs. *J. Lipid Res.* **55:** 966–977.
28. Iannotti, F. A., F. Piscitelli, A. Martella, E. Mazzarella, M. Allarà, V. Palmieri, C. Parrella, R. Capasso, and V. Di Marzo. 2013. Analysis of the "endocannabinoidome" in peripheral tissues of obese Zucker rats. *Prostaglandins Leukot. Essent. Fatty Acids.* **89:** 127–135.
29. Saz, J. M., and M. L. Marina. 2008. Application of micro- and nano-HPLC to the determination and characterization of bioactive and biomarker peptides. *J. Sep. Sci.* **31:** 446–458.
30. Houbart, V., A-C. Servais, T. D. Charlier, J. L. Pawluski, F. Abts, and M. Fillet. 2012. A validated microfluidics-based LC-chip-MS/MS method for the quantitation of fluoxetine and norfluoxetine in rat serum. *Electrophoresis.* **33:** 3370–3379.
31. Houbart, V., G. Cobraiville, F. Lecomte, B. Debrus, P. Hubert, and M. Fillet. 2011. Development of a nano-liquid chromatography on chip tandem mass spectrometry method for high-sensitivity hepcidin quantitation. *J. Chromatogr. A.* **1218:** 9046–9054.
32. Strassburg, K., A. M. L. Huijbrechts, K. A. Kortekaas, J. H. Lindeman, T. L. Pedersen, A. Dane, R. Berger, A. Brenkman, T. Hankemeier, J. van Duynhoven, et al. 2012. Quantitative profiling of oxylipins

through comprehensive LC-MS/MS analysis: application in cardiac surgery. *Anal. Bioanal. Chem.* **404:** 1413–1426.

33. Skonberg, C., A. Artmann, C. Cornett, S. H. Hansen, and H. S. Hansen. 2010. Pitfalls in the sample preparation and analysis of N-acylethanolamines. *J. Lipid Res.* **51:** 3062–3073.

34. van der Kloet, F. M., I. Bobeldijk, E. R. Verheij, and R. H. Jellema. 2009. Analytical error reduction using single point calibration for accurate and precise metabolomic phenotyping. *J. Proteome Res.* **8:** 5132–5141.

35. Zoerner, A. A., S. Batkai, M-T. Suchy, F-M. Gutzki, S. Engeli, J. Jordan, and D. Tsikas. 2012. Simultaneous UPLC-MS/MS quantification of the endocannabinoids 2-arachidonoyl glycerol (2AG), 1-arachidonoyl glycerol (1AG), and anandamide in human plasma: minimization of matrix-effects, 2AG/1AG isomerization and degradation by toluene solvent extractio. *J. Chromatogr. B Analyt. Technol. Biomed. Life Sci.* **883–884:** 161–171.

36. Rouzer, C. A., K. Ghebreselasie, and L. J. Marnett. 2002. Chemical stability of 2-arachidonylglycerol under biological conditions. *Chem. Phys. Lipids.* **119:** 69–82.

37. Nicholson, J., S. Azim, M. J. Rebecchi, W. Galbavy, T. Feng, R. Reinsel, S. Rizwan, C. J. Fowler, H. Benveniste, and M. Kaczocha. 2015. Leptin levels are negatively correlated with 2-arachidonoyl-glycerol in the cerebrospinal fluid of patients with osteoarthritis. *PLoS One.* **10:** e0123132.

38. Fortier, M., J. Tremblay-Mercier, M. Plourde, R. Chouinard-Watkins, M. Vandal, F. Pifferi, E. Freemantle, and S. C. Cunnane. 2010. Higher plasma n-3 fatty acid status in the moderately healthy elderly in southern Québec: higher fish intake or aging-related change in n-3 fatty acid metabolism? *Prostaglandins Leukot. Essent. Fatty Acids.* **82:** 277–280.

39. Meijerink, J., M. Balvers, and R. Witkamp. 2013. N-acyl amines of docosahexaenoic acid and other n-3 polyunsatured fatty acids - from fishy endocannabinoids to potential leads. *Br. J. Pharmacol.* **169:** 772–783.

40. Plourde, M., R. Chouinard-Watkins, M. Vandal, Y. Zhang, P. Lawrence, J. T. Brenna, and S. C. Cunnane. 2011. Plasma incorporation, apparent retroconversion and β-oxidation of 13C-docosahexaenoic acid in the elderly. *Nutr. Metab. (Lond.).* **8:** 5.